

Synthesis, structure and luminescent property of a new hybrid solid based on Keggin anions and silver-organonitrogen fragments

Jian Lü^{a,b}, Fu-Xian Xiao^{a,b}, Lin-Xi Shi^a, Rong Cao^{a,*}

^aState Key Laboratory of Structural Chemistry, Fujian Institute of Research on the Structure of Matter, Chinese Academy of Sciences, Fujian, Fuzhou 350002, PR China

^bGraduate School, Chinese Academy of Sciences, Beijing 100039, PR China

Received 26 August 2007; received in revised form 20 November 2007; accepted 26 November 2007

Available online 9 January 2008

Abstract

A new hybrid solid, $\{\text{Ag}(\text{phen})_2\}_2\{\text{[Ag}(\text{phen})_2\text{PMo}_{12}\text{O}_{40}]\}$ (phen = 1,10-phenanthroline) **1**, constructed from one-electron-reduced mono-supported α -Keggin polyanions and silver-phenanthroline fragments via either covalent bonds or supramolecular interactions, is described. In the structure of **1**, mono-supported $\{\text{Ag}(\text{phen})[\text{PMo}_{12}\text{O}_{40}]\}^{3-}$ polyanions are connected by $\{\text{Ag}(\text{phen})\}^+$ linking fragments to form a hybrid chain structure with engrafted phen ligands. $\{\text{Ag}(\text{phen})_2\}^+$ counter-cations occur in pairs trapping in strong inter-chain π - π stacking to form a three-dimensional supramolecular framework. Luminescent investigation of the compound indicates that **1** displays fascinating orange luminescent property at ambient temperature.

© 2007 Elsevier Inc. All rights reserved.

Keywords: Polyoxometalate; Silver; Organonitrogen; Supramolecular; Keggin

1. Introduction

Polyoxometalate (POM) chemistry has recently been undergoing a vigorous period characterized by a large amount of solid-state materials with distinctive topological structures and versatile applications in given fields [1–5], especially in optical [4] and magnetic areas [5]. The POM moieties observed in these complexes include classical POMs [6–10], newly founded POMs [11–15], and modified POM derivatives [16–21]. In the field of modified POMs, materials based on substituted, capped, and supported POMs become extraordinarily promising because of their changeable and controllable structures as well as their predominant properties introduced by modifying moieties [5,7,9,13]. Recently, crystal engineering of hybrid materials is realizable through the so-called “building-block” concept [22–27], and the modified POMs have been widely used as functional building blocks to construct solid-state materials [18–21]. Consequently, many polymeric solids based on substituted or capped POMs have been success-

fully isolated hitherto [18–21,28–30]. However, although hybrid solids based on supported POMs were infrequently isolated, to the best of our knowledge, only two examples of one-dimensional (1-D) structures constructed from mono-supported Dawson-type clusters and alkaline-earth metal-organic fragments were documented [31,32].

It is well investigated that symmetric POM moieties are easy to be used as efficient building blocks in constructing extended structures [7–10]. Substituted POMs often display similar symmetries to the parent POMs because of their distinctive structural features of direct group substitution. Capped POMs also possess high symmetries due to the particular way that the capping moieties distributed on the surface of POM hosts. In comparison with substituted and capped POM clusters, supported POMs usually display lower symmetries, and it may be the reason that hybrid solids based on supported POMs are rarely discovered. In this sense, structural characterization of extended structures based on supported POMs is especially significant.

Herein, we report the synthesis, structure and luminescent property of a new hybrid solid based on mono-supported Keggin clusters and silver-organonitrogen fragments, formulated as $\{\text{Ag}(\text{phen})_2\}_2\{\text{[Ag}(\text{phen})_2\text{PMo}_{12}\text{O}_{40}]\}$

*Corresponding author. Fax: +86 591 8379 6710.

E-mail address: rcao@fjirsm.ac.cn (R. Cao).

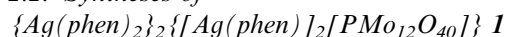
(phen = 1,10-phenanthroline) **1**. X-ray crystallography reveals that **1** possesses a three-dimensional (3-D) supramolecular structure containing 1-D hybrid chains based on mono-supported Keggin clusters, in which the silver-phenanthroline fragments play versatile structural roles. It is the first example of an extended architecture based on supported POM clusters and transition metal complexes. It is also noteworthy that **1** displays fascinating orange luminescent property at ambient temperature.

2. Experimental section

2.1. General

All chemicals were commercially purchased and used without purification. Elemental analyses (C, H, N) were carried on an Elementar Vario EL III analyzer. Ag and Mo were determined by a Jobin Yvon Ultima2 ICP atomic emission Spectrometer. Infrared (IR) spectrum was recorded with Perkin Elmer Spectrum One as KBr pellets in the range 400–4000 cm^{-1} . X-ray powder diffraction (XRPD) was performed with a Rigaku DMAX 2500 diffractometer. Electron paramagnetic resonance (EPR) was performed with a Bruker-ER-420 X-band recorder. UV–Vis spectrum was recorded with Lambda35 and Lambda900 (Perkin Elmer, USA) spectrometers. Luminescence spectrum for the solid samples was recorded with a PE LS55 fluorescence spectrophotometer. Single crystal X-ray diffraction was carried on a Bruker SMART 1K diffractometer.

2.2. Syntheses of



A mixture of $(\text{NH}_4)_6\text{Mo}_7\text{O}_{24}\cdots 4\text{H}_2\text{O}$, H_3PO_4 , AgNO_3 , 1,10-phenanthroline and H_2O in the molar ratio of 2:1:2:2:550 was stirred for 20 min in air. The mixture was then transferred to a Teflon-lined autoclave (20 mL) and kept at 140 °C for 3 days. After slow cooling to room temperature within 2 days, dark colored block crystals of **1** were filtered off, washed with distilled water and dried in air to give a yield of ca. 40% (based on Mo). Anal. Calcd. for $\text{C}_{72}\text{H}_{48}\text{Ag}_4\text{Mo}_{12}\text{N}_{12}\text{O}_{40}\text{P}$ (%): C, 25.93; H, 1.45; N, 5.04; Ag, 12.94; Mo, 34.52; found (%): C, 25.51; H, 1.26; N, 5.12; Ag, 12.21; Mo, 33.93. IR characteristics (KBr, cm^{-1}): 3442, 3057m, 1618, 1587, 1570w, 1508, 1421m, 1219, 1144w, 1051m, 947, 874, 847, 793, 729s, 633, 509m.

2.3. X-ray structure determination

The data were collected on a Bruker SMART 1000 CCD diffractometer equipped with graphite-monochromated Mo $K\alpha$ radiation with a radiation wavelength of 0.71073 Å by using the ω -scan technique. Absorption correction was performed using the SADABS program [33]. Structure was solved by direct methods and refined on F^2 by full matrix least-squares using the SHELXTL-97

Table 1
Crystal data and structure refinement for Compound **1**

Empirical formula	$\text{C}_{72}\text{H}_{48}\text{Ag}_4\text{Mo}_{12}\text{N}_{12}\text{O}_{40}\text{P}$
Formula weight	3334.95
Temperature (K)	293(2)
Wavelength (Å)	0.71073
Crystal system	Monoclinic
Space group	$C2/c$
a (Å)	10.9134(5)
b (Å)	47.545(2)
c (Å)	17.1692(8)
β (°)	106.3110(1)
Volume (Å ³)	8550.1(7)
Z	4
Goodness-of-fit on F^2	1.042
Final R indices [I and $2\sigma(I)$]	$R_1^a = 0.0725$, $wR_2^b = 0.1306$
Indices (all data)	$R_1^a = 0.1209$, $wR_2^b = 0.1480$

$$^a R_1 = \frac{\sum \|F_o\| - |F_c|}{\sum \|F_o\|}$$

$$^b wR_2 = \left\{ \frac{\sum [w(F_o^2 - F_c^2)^2]}{\sum [w(F_o^2)]} \right\}^{1/2}$$

Table 2
Selected bond lengths and angles for Compound **1**

Bond lengths			
Ag(1)–N(2)	2.226(1)	Ag(2)–N(5)#1	2.320(1)
Ag(1)–N(4)	2.287(1)	Ag(2)–N(5)	2.320(1)
Ag(1)–N(3)	2.392(1)	Ag(2)–O(20)#2	2.603(8)
Ag(1)–N(1)	2.440(1)	Ag(2)–O(20)#1	2.603(8)
Ag(3)–N(6)#3	2.329(1)	Mo(1)–O(1)	1.671(7)
Ag(3)–N(6)	2.329(1)	Mo(1)–O(1)	1.839(7)
Ag(3)–O(2)#3	2.399(7)	Mo(1)–O(2)	1.867(7)
Ag(3)–O(2)	2.399(7)	Mo(1)–O(1)	1.983(7)
Mo(2)–O(5)	1.679(8)	Mo(1)–O(2)	1.988(7)
Mo(2)–O(2)#2	1.887(7)	Mo(3)–O(2)	1.667(8)
Mo(2)–O(2)	1.887(7)	Mo(3)–O(2)	1.836(7)
Mo(2)–O(1)	1.892(8)	Mo(3)–O(1)	1.863(7)
Mo(2)–O(1)	1.942(7)	Mo(3)–O(1)	1.979(7)
Mo(2)–O(2)#1	1.950(7)	Mo(3)–O(1)	2.006(7)
Mo(4)–O(4)	1.679(7)	Mo(5)–O(6)	1.667(7)
Mo(4)–O(1)	1.849(8)	Mo(5)–O(1)	1.818(7)
Mo(4)–O(2)	1.852(7)	Mo(5)–O(2)	1.916(7)
Mo(4)–O(2)#2	1.967(7)	Mo(5)–O(7)#1	1.933(7)
Mo(4)–O(2)	1.967(7)	Mo(5)–O(16)	1.980(7)
Mo(4)–O(1)#1	1.980(8)	P(1)–O(9)#1	1.537(7)
Mo(6)–O(8)	1.675(7)	P(1)–O(9)	1.537(7)
Mo(6)–O(2)	1.848(7)	P(1)–O(3)	1.538(7)
Mo(6)–O(7)	1.848(7)	P(1)–O(3)#1	1.538(7)
O(15)#1...H...C(9)D	3.401(2)	O(5)#1...H...C(17)	3.199(2)

Symmetry transformations used to generate equivalent atoms: #1 $-x, y, -z + 3/2$; #2 x, y, z ; #3 $-x + 1, y, -z + 3/2$.

program package [34]. All non-hydrogen atoms were refined anisotropically. The organic hydrogen atoms were positioned geometrically. Structure solution and refinement based on 8138 independent reflections gave R_1 (wR_2) = 0.0725 (0.1306). A summary of the crystallographic data and structural determination for **1** is provided in Table 1. Selected bonds are listed in Table 2.

3. Results and discussion

3.1. Crystal Structure of

$\{Ag(phen)_2\}_2\{[Ag(phen)]_2[PMo_{12}O_{40}]\}_1$

The crystal structure of **1** is assembled from mono-supported α -Keggin polyanion clusters, $\{[Ag(phen)][PMo_{12}O_{40}]\}^{3-}$, covalently attached by $[Ag(phen)]^+$ complexes to form a 1-D hybrid chain, and the 1-D chains are extended to a 3-D supramolecular framework via extensive hydrogen bonding and π - π interactions. The well-known α -Keggin cluster in **1** consists of four groups of tri-metallic $\{MoO_6\}_3$ units. Each $\{MoO_6\}$ octahedron in one trimetallic unit shares an edge with a neighboring one, and the $\{MoO_6\}_3$ units link together via corner sharing $\{MoO_6\}$ octahedra to form a cluster cage with a $\{PO_4\}$ tetrahedron located in the center of the host cage. There are three crystallographically independent silver sites with two of them half-occupied in the asymmetric unit (Fig. S1). The Ag(1) atom, residing in roughly distorted tetrahedral environment, coordinates to four nitrogen donors from two phen ligands. The Ag(2) and Ag(3) sites are both defined by two N donors from a phen ligand and two surface O atoms of Keggin clusters to finish their slightly distorted tetrahedral coordination environment. The only difference is that Ag(2) coordinates to two μ_2 -O atoms from two $\{(MoO_6)_3\}$ units in a Keggin cluster, whereas Ag(3) links with two μ_2 -O atoms from two Keggin clusters. The Ag–N bonds range from 2.231 to 2.449 Å, and Ag–O bonds are 2.597 and 2.400 Å, respectively.

The mono-supported α -Keggin polyanion in **1**, $\{[Ag(phen)][PMo_{12}O_{40}]\}^{3-}$ shown in Fig. 1a, is constructed from a one-electron-reduced α -Keggin cluster supported with a $\{Ag(phen)\}^+$ fragment via two surface bridging O atoms which belong to two different trimetallic subunits. Such polyanion clusters are further connected together by means of the covalent linkage of the same $\{Ag(phen)\}^+$ fragments to form a hybrid chain along the *a*-axis (Fig. 1b). The Keggin clusters locate in line and the aromatic rings of phen ligands point perpendicularly out the chain. Surprisingly, the $[Ag(phen)_2]^+$ counter-cations assemble in pairs with weak interactions between two Ag centers of 3.551 Å. Adjacent 1-D chains are bolted together by the complex pairs generating a regular two-dimensional (2-D) layer via strong π - π interactions (Fig. 2a). The closest distance between parallel aromatic rings is 3.384 Å. The 2-D layers are connected into a 3-D framework via extensive hydrogen interactions between surface O atoms of Keggin clusters and H atoms of aromatic rings (Fig. 2b). Typical hydrogen bonds represented by O15H...H9D...C9D and O5H...H17F...C17F are 3.401 and 3.199 Å, respectively.

Typically, metal complex subunits in hybrid solids can act as decorating, linking, or counter-cation fragments. In the structure of **1**, silver-phenanthroline fragments display all three above-mentioned characteristics surprisingly. To the best of our knowledge, it is the first time that metal complexes show versatile structural features in a single structure.

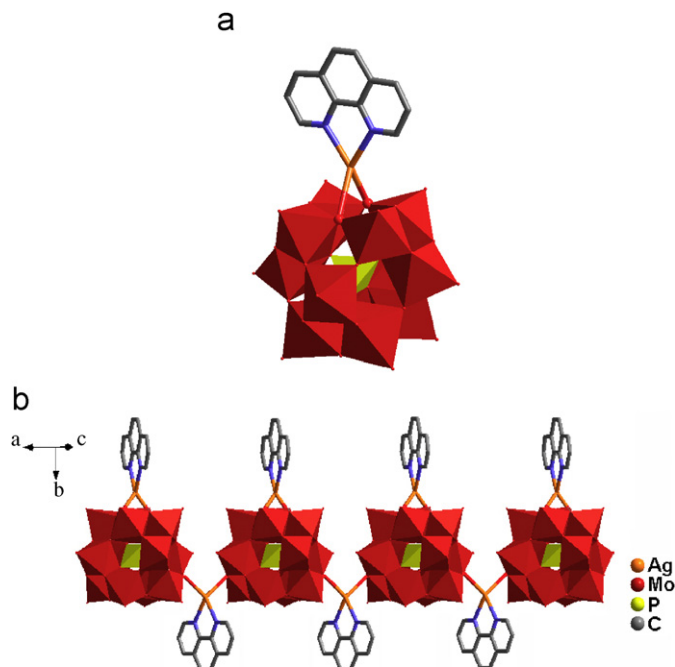


Fig. 1. A polyhedral presentation of (a) the mono-supported α -Keggin cluster in **1**, and (b) the 1-D chain showing the coordination of $\{xAg(phen)\}^+$ fragments on the Keggin clusters. H atoms attached to phenanthroline ligand are omitted for clarity.

3.2. Discussion

The formation of an extended structure based on mono-supported Keggin clusters is assigned to the synergistic interaction between the cluster units and metal-organic fragments. It is presumed that POM clusters with higher symmetric structures are more stable and easier to meet the coordination abilities of complex fragments to construct polymeric structures than POMs with lower symmetries. It may be the possible reason that examples of extended structures based on supported POM clusters, one kind of low symmetric moieties, are far less been documented, in comparison with the structures based on classical Keggin-, Anderson-, or Dawson-type polyanions and high symmetric modified POM clusters. The symmetry of mono-supported POM moiety in **1** is lowered due to the covalent attachment of a silver-phenanthroline fragment, which makes it difficult to construct extended structures by means of complex linkages. However, the same linking complex units as the supporting fragments display a triangle arrangement on the surface of a Keggin cluster. Such kind of linking fashion transforms the asymmetric mono-supported α -Keggin moiety to a pseudo-*Td* symmetry unit (considering the Keggin moiety and three $[Ag(phen)]^+$ fragments attached on it). The coordination preference to form a high symmetric structure is probably one of the key factors to get the final structure. It is also believed that the $\{Ag(phen)_2\}_2^{2+}$ complex pairs play a vital role in stabilization the 1-D hybrid chain as the mean distance of adjacent

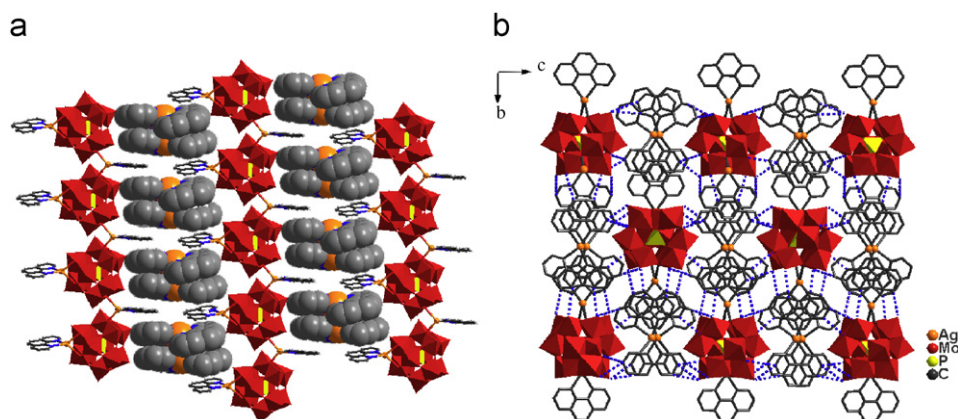


Fig. 2. (a) Packing of the 2-D network showing the π - π interactions between 1-D chains and $\{\text{Ag}(\text{phen})_2\}_2^{2+}$ pairs. $\{\text{Ag}(\text{phen})_2\}_2^{2+}$ subunits are shown in spacefill fashion for clarity. (b) The 3-D supramolecular framework of **1**, exhibiting the linkage of hydrogen bonds in intra- and interlamellar regions along a -axis.

parallel aromatic rings decorated on the 1-D chains is 10.9 Å, which is quite long for a lone $\{\text{Ag}(\text{phen})_2\}^+$ unit to be involved in π - π interactions. The formation of $\{\text{Ag}(\text{phen})_2\}_2^{2+}$ pairs fences off the voids into effective intervals for the formation of π - π stacking. It is therefore believed the silver-phenanthroline fragments play extremely important roles in the structure.

3.3. XRPD, IR, EPR, and UV-Vis-near-IR Spectra

The experimental and simulated XRPD patterns of compound **1** are shown in Fig. S2. Their peak positions are in good agreement with each other, indicating the phase purity of the product. The IR spectrum (Fig. S3) of compound **1** displays a series of complicated bands in the range of 400–1800 cm^{-1} . The strong bands in 800–1100 cm^{-1} are characteristics of Keggin clusters and the bonds in 1680–1100 cm^{-1} are attributable to the organic ligands. It should be noted that the asymmetric $\nu_{\text{Mo-O}}$ mode for $[\text{PMo}_{12}\text{O}_{40}]^{4-}$ is observed at 947 cm^{-1} showing a red-shifted energy of 15 cm^{-1} compared with the characteristic vibrational bond of $[\text{PMo}_{12}\text{O}_{40}]^{3-}$ cluster (962 cm^{-1}). The red shifts of the asymmetric $\nu_{\text{Mo-O}}$ mode is assigned to the one-electron reduction of Keggin cluster in **1** which is accordant with the characteristic Mo-O stretching of reduced Keggin cluster documented in the literature [35], and the force constant of Mo-O stretching mode was found to decrease by the one-electron reduction due to electron delocalization in the cluster. The EPR spectrum of **1** (Fig. S4) at room temperature shows a signal of $g = 2.047$, which is a little larger than the reported values for Mo^{5+} possibly due to the electron delocalization and spin-orbital interaction [36,37]. It further demonstrates the existence of reduced Mo(V) centers in **1**. The UV-Vis spectrum of **1** (Fig. S5) displays two intense absorption peaks at 265 and 310 nm, assigning to the adsorption of phen ligands. A shoulder peak at 280 nm is probably due to the adsorption of the modified Keggin cluster. The UV-Vis-near-IR spectrum of **1** (Fig. S6) shows

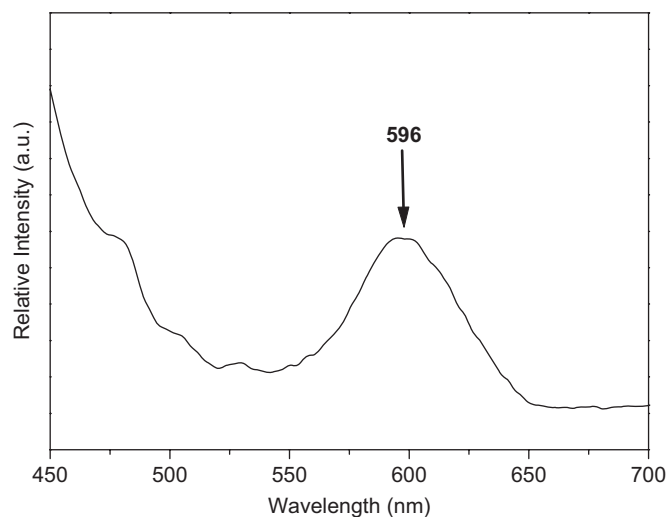


Fig. 3. Solid-state emission spectrum of **1** at room temperature.

absorption bands at 960, 1150, and 1190 nm. In comparison with the spectrum of phen ligands, bands at 960 and 1150 nm belong to the adsorption of phen. The low-energy absorption at 1190 nm is attributed to the intervalence transition from Mo(V) to Mo(VI) through the Mo-O-Mo bond within the cluster and the d - d transitions of Mo(V) octahedra according to the literatures [35].

3.4. Luminescent property

The emission spectrum of compound **1** in the solid state at room temperature was investigated, as plotted in Fig. 3. The hybrid solid **1** displays fascinating orange luminescent property at ambient temperature. Upon excitation at ca. 420 nm, emission band of **1** at ca. 596 nm is observed. The emission is tentatively assigned as originating from the mixed ligand-to-ligand charge-transfer (LLCT) and/or metal-metal-to-ligand charge-transfer (MMLCT) taking into consideration the strong π - π interactions and weak Ag...Ag interactions in **1** [35,36]. Considerable fluorescent

intensity decrease of sample **1** is assigned significant connection of π – π interactions in the present structure [37]. The possible reason is that the energy received by ligand is partially lost. It is noteworthy that this low energy luminescence is unusual, in comparison with the large numbers of blue emission Ag(I) coordination polymers [38,39] and representing a singular example with orange fluorescent property for potential uses as photoluminescence materials.

4. Conclusions

In short, we have prepared and characterized a novel 3-D supramolecular structure containing 1-D hybrid chains based on mono-supported Keggin clusters. The successful preparation of **1** opens up a possible way to prepare hybrid solid materials based on supported POM building blocks. The structural novelty represented by simultaneous occurrence of supporting, linking and countering complex fragments in **1** not only proves again the crucial role metal complexes play in hybrid solids [40] but also dramatically leads to the research efforts in the system of novel hybrid materials based on supported POMs.

Acknowledgments

This work was financially supported by 973 Program (2006CB932900), NSFC (90206040, 20325106, 50472021, 20731005), NSF of Fujian Province (2005HZ01-1, E0520003), Fujian Key Laboratory of Nanomaterials (2006L2005), “The Distinguished Oversea Scholar Project” and, “One Hundred Talent Project” and key project from CAS. J. L. thanks Prof. Ulrich Kortz for helpful discussion on this study.

Appendix A. Supplementary data

Crystallographic data in CIF format have been deposited at the Cambridge Crystallographic Data Centre with CCDC numbers **624829**. Copies of this information may be obtained free of charge from the Director, CCDC, 12 Union Road, Cambridge CB2 1EZ, UK (fax: +44 1223 336033; e-mail: deposit@ccdc.cam.ac.uk; or <http://www.ccdc.cam.ac.uk>). Supplementary data associated with this article can be found in the online version.

Appendix B. Supplementary data

Supplementary data associated with this article can be found in the online version at [doi:10.1016/j.jssc.2007.11.026](https://doi.org/10.1016/j.jssc.2007.11.026).

References

- [1] I.V. Kozhevnikov, Chem. Rev. 98 (1998) 171.
- [2] N. Mizuno, M. Misono, Chem. Rev. 98 (1998) 199.
- [3] J.T. Rhule, C.L. Hill, D.A. Judd, R.F. Schinazi, Chem. Rev. 98 (1998) 327.
- [4] T. Yamase, Chem. Rev. 98 (1998) 307.
- [5] E. Coronado, C.J. Gómez-García, Chem. Rev. 98 (1998) 273.
- [6] I. Bar-Nahum, K.V. Narasimhulu, L. Weiner, R. Neumann, Inorg. Chem. 44 (2005) 4900.
- [7] H. An, Y. Li, E. Wang, D. Xiao, C. Sun, L. Xu, Inorg. Chem. 44 (2005) 6062.
- [8] Y.-P. Ren, X.-J. Kong, L.-S. Long, R.-B. Huang, L.-S. Zheng, Cryst. Growth Design 6 (2006) 572.
- [9] J.-X. Chen, T.-Y. Lan, Y.-B. Huang, C.-X. Wei, Z.-S. Li, Z.-C. Zhang, J. Solid State Chem. 179 (2006) 1904.
- [10] M. Wei, C. He, W. Hua, C. Duan, S. Li, Q.J. Meng, J. Am. Chem. Soc. 128 (2006) 13318.
- [11] A. Dolbecq, P. Mialane, L. Lisnard, J. Marrot, F. Sécheresse, Chem. Eur. J. 9 (2003) 2914.
- [12] D. Laurencin, R. Villanneau, P. Herson, R. Thouvenot, Y. Jeannin, A. Proust, Chem. Commun. (2005) 5524.
- [13] B.S. Bassil, S. Nellutla, U. Kortz, A.C. Stowe, J. van Tol, N.S. Dalal, B. Keita, L. Nadjo, Inorg. Chem. 44 (2005) 2659 (and references therein).
- [14] T.M. Anderson, R. Cao, E. Slonkina, B. Hedman, K.O. Hodgson, K.I. Hardcastle, W.A. Neiwert, S. Wu, M.L. Kirk, S. Knottenbelt, E.C. Depperman, B. Keita, L. Nadjo, D.G. Musaev, K. Morokuma, C.L. Hill, J. Am. Chem. Soc. 127 (2005) 11948.
- [15] B. Botar, P. Kögerler, A. Müller, R. Garcia-Serresd, C.L. Hill, Chem. Commun. (2005) 5621.
- [16] M. Yuan, Y.G. Li, E.B. Wang, C.G. Tian, L. Wang, C.W. Hu, N.H. Hu, H.Q. Jia, Inorg. Chem. 42 (2003) 3670.
- [17] F. Hussain, U. Kortz, R.J. Clark, Inorg. Chem. 43 (2004) 3237 (and references therein).
- [18] B. Godin, J. Vaissermann, P. Herson, L. Ruhlmann, M. Verdager, P. Gouzerh, Chem. Commun. (2005) 5624.
- [19] N. Belai, M.T. Pope, Chem. Commun. (2005) 5760.
- [20] N. Leclerc-Laronze, J. Marrot, G. Hervé, Inorg. Chem. 44 (2005) 1275.
- [21] S.-T. Zheng, J. Zhang, G.-Y. Yang, Inorg. Chem. 44 (2005) 2426.
- [22] H. Li, M. Eddaoudi, M. O’Keeffe, O.M. Yaghi, Nature 402 (1999) 276.
- [23] S.S.-Y. Chui, S.M.-F. Lo, J.P.H. Charmant, A.G. Orpen, I.D. Williams, Science 283 (1999) 1148.
- [24] B. Chen, M. Eddaoudi, S.T. Hyde, M. O’Keeffe, O.M. Yaghi, Science 291 (2001) 1021.
- [25] M. Eddaoudi, J. Kim, N. Rosi, D. Vodak, D.V. Wachter, M. O’Keeffe, O.M. Yaghi, Science 295 (2002) 469.
- [26] N.L. Rosi, J. Eckert, M. Eddaoudi, D.T. Vodak, J. Kim, M. O’Keeffe, O.M. Yaghi, Science 300 (2003) 1127.
- [27] S.L. James, Chem. Soc. Rev. 32 (2003) 276.
- [28] J.-P. Wang, X.-Y. Duan, X.-D. Du, J.-Y. Niu, Cryst. Growth Design 6 (2006) 2266.
- [29] P. Mialane, A. Dolbecq, F. Sécheresse, Chem. Commun. (2006) 3477.
- [30] C.-M. Liu, D.-Q. Zhang, M. Xiong, D.-B. Zhu, Chem. Commun. (2002) 1416.
- [31] J.-Y. Niu, D.-J. Guo, J.-W. Zhao, J.-P. Wang, New J. Chem. 28 (2004) 980.
- [32] J.-Y. Niu, D.-J. Guo, J.-P. Wang, J.-W. Zhao, Cryst. Growth Design 4 (2004) 241.
- [33] G.M. Sheldrick, SADABS, Program for Empirical Absorption Correction of Area Detector Data, University of Göttingen, 1996.
- [34] G.M. Sheldrick, SHELXS-97, Program for Crystal Structure Solution and Refinement, University of Göttingen, 1997.
- [35] H. Tannai, K. Tsuge, Y. Sasaki, O. Hatozaki, N. Oyamab, Dalton Trans. (2003) 2353.
- [36] V.W.-W. Yam, E.C.-C. Cheng, N. Zhu, New J. Chem. 26 (2002) 279.

- [37] S.Q. Liu, T. Kuroda-Sowa, H. Konaka, Y. Suenaga, M. Maekawa, T. Mizutani, G.L. Ning, M. Munakata, *Inorg. Chem.* 44 (2005) 1031.
- [38] R.P. Feazell, C.E. Carson, K.K. Klausmeyer, *Eur. J. Inorg. Chem.* (2005) 3287.
- [39] Y.J. Kang, C. Seward, D.T. Song, S.N. Wang, *Inorg. Chem.* 42 (2003) 27891.
- [40] P.J. Hagrman, D. Hagrman, J. Zubieta, *Angew. Chem. Int. Ed. Engl.* 38 (1999) 2638.